On the Mechanism and Stereoselectivity of the Copper(I)-Catalyzed Cyclopropanation of Olefins − A Combined Experimental and Density Functional Study[‡]

Michael Bühl,*[a] Frank Terstegen,[a] Frank Löffler,[b] Bernd Meynhardt,[b] Stefanie Kierse,[b] Michael Müller,[c] Christian Näther,[d] and Ulrich Lüning*[b]

Keywords: Ab initio calculations / Carbenes / Carbene complexes / Catalysis / Copper

The mechanism of copper(I)-catalyzed olefin cyclopropanation with diazomethanes has been studied at the BP86/AE1 level of density-functional theory. For the model system Cu(diazabutadiene)$^+$ + ethene + diazomethane, copper carbene complexes are confirmed as viable intermediates, with rate-determining barriers of the order of 25 kcal/mol (energies including zero-point corrections) or 14 kcal/mol (when entropic contributions are included). For another model system, Cu(2,9-dimethyl-1,10-phenanthroline)$^+$ + styrene + diazoacetate, very small *anti*/*syn* selectivities (resulting in *trans*/*cis*-cyclopropanes) have been found both computationally and experimentally. Cu(carbene) complexes with macrocyclic phenanthroline-based ligands **1** (aryl bridgeheads and ether linkages) and **2** (calix[6]arene) have been optimized at the BP86/SDD level. A qualitative explanation for the *trans* selectivity observed with **1**, based on the tilted, cleft-like conformation of **1**·(CuCHCO$_2$Me)$^+$, is put forward. Similar conformations are found in structures of related acyclic mono- and diarylphenanthrolines (either free or complexed with Cu^{2+} or Pd^{2+}), which have been determined by X-ray crystallography. The observed *cis* selectivity of **2** is probably related to the fact that in **2**·(CuCHCO$_2$Me)$^+$ the calixarene macrocycle effectively blocks one hemisphere of the catalyst.

Introduction

Selective cyclopropanation of alkenes by diazo compounds, catalyzed by transition metal complexes, can be carried out if suitable ligands are chosen. Stereoselective and enantioselective cyclopropanations are thus possible.[1] For example, if concave 1,10-phenanthrolines are used as ligands in a copper(I)-based catalyst, both *anti*- and *syn*-cyclopropanes can be obtained with good selectivities, depending on the nature of the concave ligand.[1m] The bimacrocyclic 2,9-diaryl-1,10-phenanthrolines **1** predominantly give *anti*-cyclopropanes (up to 140:1; indene and *tert*-butyl diazoacetate), while 1,10-phenanthrolines **2** are *syn*-selective (14:86; **2a**, indene and methyl diazoacetate) (Scheme 1). The different selectivities are intriguing because of the apparent similarity of the two classes of bimacrocyclic ligands.

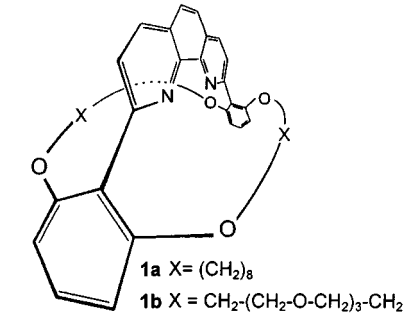

Scheme 1

To obtain a deeper understanding of the underlying mechanisms, a density-functional study of the cyclopropanation reaction has been carried out. For this task, the potential energy surface was explored using model ligand **3** instead of the bimacrocyclic ligands **1** and **2**. Key intermediates and transition structures were recomputed, em-

[‡] Concave Reagents 34. − Part 33: Ref.[8]
[a] Max-Planck-Institut für Kohlenforschung, Kaiser-Wilhelm-Platz 1, 45470 Mülheim an der Ruhr, Germany
Fax: (internat.) + 49-(0)208/306-2996
E-mail: buehl@mpi-muelheim.mpg.de
[b] Institut für Organische Chemie der Christian-Albrechts-Universität zu Kiel, Olshausenstrasse 40, 24098 Kiel, Germany
Fax: (internat.) + 49-(0)431/880-1558
E-mail: luening@oc.uni-kiel.de
[c] Gewerbliches Institut für Umweltanalytik GmbH, Waidplatzstrasse 8, 79331 Teningen, Germany
Fax: (internat.) + 49-(0)7663/4039
E-mail: info@giu-umwelt.de
[d] Institut für Anorganische Chemie der Christian-Albrechts-Universität zu Kiel, Olshausenstrasse 40, 24098 Kiel, Germany
Fax: (internat.) + 49-(0)431/880-1520
E-mail: cnaether@ac.uni-kiel.de

  1434−193X/01/0611−2151 $ 17.50+.50/0

ploying the larger model ligand 2,9-dimethyl-1,10-phenanthroline (**4**). In addition, **4** and related compounds (2-aryl-1,10-phenanthroline **5a**, 2,9-diaryl-1,10-phenanthrolines **6b**–**d**) were also investigated experimentally, in order to correlate the calculations with the selectivity measurements (Scheme 2).

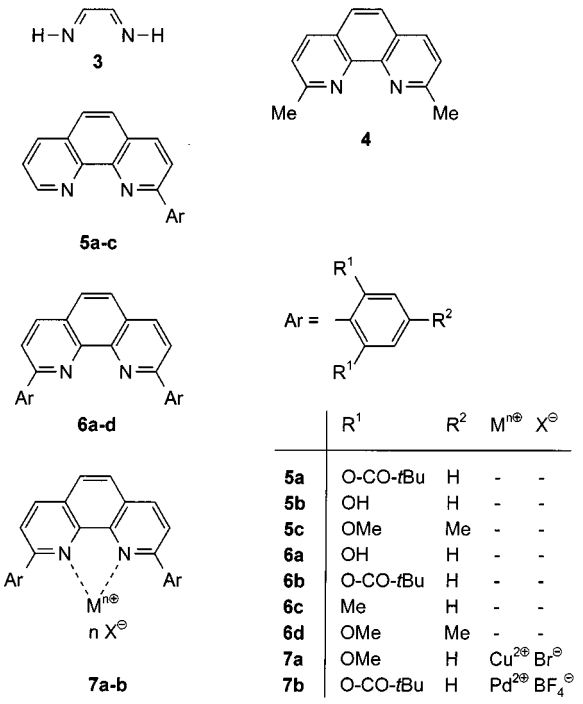

	R^1	R^2	$M^{n\oplus}$	$X^{\ominus}$
5a	O-CO-*t*Bu	H	-	-
5b	OH	H	-	-
5c	OMe	Me	-	-
6a	OH	H	-	-
6b	O-CO-*t*Bu	H	-	-
6c	Me	H	-	-
6d	OMe	Me	-	-
7a	OMe	H	$Cu^{2\oplus}$	$Br^{\ominus}$
7b	O-CO-*t*Bu	H	$Pd^{2\oplus}$	$BF_4^{\ominus}$

Scheme 2

Results and Discussion

1. 1,4-Diazabutadiene Complexes

The simplest model for **1** and **2** is 1,4-diazabutadiene (DAB) (**3**). Even though **3** lacks the aromatic system of the real ligands, an initial qualitative assessment of the energetics of possible intermediates should be possible. Thus, a detailed study of the **3**·Cu^+ (**8**) + C_2H_4 + CH_2N_2 potential energy surface was carried out at the BP86/AE1 level; important minima are displayed in Figure 1.[2] The first and the last copper model complexes in this sequence are identical and the energy difference originates from the thermodynamic driving force on going from reactants to products. For the isolated system, the cyclopropane complex **3**·Cu(*c*-$C_3H_6)^+$ (or, rather, a weak complex thereof with N_2, **14**) is lowest in energy and is probably the resting state in the catalytic cycle.

This complex appears to reside in a fairly deep energy well, and on first glance one would expect the limiting step to be cyclopropane dissociation from this resting state **14**, with formation of free **3**·Cu^+. However, this process is highly endothermic and is unlikely to occur in the real systems in solution.[3] There are, however, alternative mechanisms starting from **3**·Cu(*c*-$C_3H_6)^+$ (**14**) to complexes between copper and reactants, namely associative replacement of cyclopropane with either C_2H_4 or CH_2N_2. For instance, the reaction

3·Cu(*c*-$C_3H_6)^+$ + CH_2N_2 → *c*-C_3H_6 + **3**·Cu$(CH_2N_2)^+$
ΔE = −14.8 kcal/mol (−13.2 incl. *ZPE*)

can proceed through an intermediate with both ligands attached to the copper ion, **3**·Cu(*c*-C_3H_6)$(CH_2N_2)^+$ (not shown in Figure 1). This intermediate is −18.5 kcal/mol (−16.4 incl. *ZPE*) below **14** + CH_2N_2. Since barriers for simple ligand addition and dissociation are presumably small, the copper complexes can rapidly exchange product with fresh reactant. The rate-determining step will thus be elsewhere on the energy surface.

The diazomethane complex **3**·Cu$(CH_2N_2)^+$ (**10a**), after rearrangement to the slightly less stable *C*-coordinated form **10b**, can lose N_2 with formation of the carbene complex **3**·Cu$(CH_2)^+$ (**11**), a process which is endothermic by 16.1 kcal/mol. The transition state for this step has been located (not shown in Figure 1); only a little extra activation is required, and a total barrier of 18.6 kcal/mol is obtained. From the carbene complex, addition of ethene and formation of the cyclopropane resting state essentially goes downhill (path I, upper part of Figure 1).

As an alternative to this path, the cyclopropane in **3**·Cu(*c*-$C_3H_6)^+$ (**14**) can be replaced associatively by ethene according to

3·Cu(*c*-$C_3H_6)^+$ + C_2H_4 → *c*-C_3H_6 + **3**·Cu$(C_2H_2)^+$
ΔE = −16.9 kcal/mol (−15.0 incl. *ZPE*)

The ethene complex is slightly favored thermodynamically over the diazomethane complex. The former can add a diazomethane molecule, with formation of **3**·Cu$(C_2H_4)(CH_2N_2)^+$ (**13**), followed by loss of N_2 (path II, lower part of Figure 1). The latter process is endothermic by 22.7 kcal/mol, and virtually no additional activation energy is necessary that is the transition state is very similar in energy to the separated products, N_2 + **3**·Cu$(CH_2)(C_2H_4)^+$ (**12**). The highest point on path II is the transition state from **12** to **3**·Cu(*c*-$C_3H_6)^+$ (**14**), 48.2 kcal/mol above **14** (24.7 kcal/mol above **13**, not shown in Figure 1). This transition state, which is also attained on path I (in which, however, it is not the highest point, since it is lower in energy than the free carbene complex) is the one that determines the stereoselectivity (see below). Again, only little further activation is needed once **3**·Cu$(CH_2)(C_2H_4)^+$ (**12**) has been formed.

Addition of ethene to **3**·Cu$(CH_2N_2)^+$ (**10**) connects paths I and II, thereby circumventing the pristine carbene complex. Once more, this process is virtually free of activation on the potential energy surface. Since the energy decreases considerably during this process (by 17 kcal/mol, Figure 1), path II should be strongly favored. Because of the variation in particle numbers, however, inclusion of thermal and, in particular, entropic effects is essential. Table 1 summarizes the relevant thermodynamic data.

As is the case on the potential energy surface, dissociation of cyclopropane from **3**·Cu(*c*-$C_3H_6)^+$ (**14**) is a highly endergonic process on the free energy surface. Complex **3**·Cu$(C_2H_4)(CH_2N_2)^+$ (**13**) remains the most stable interme-

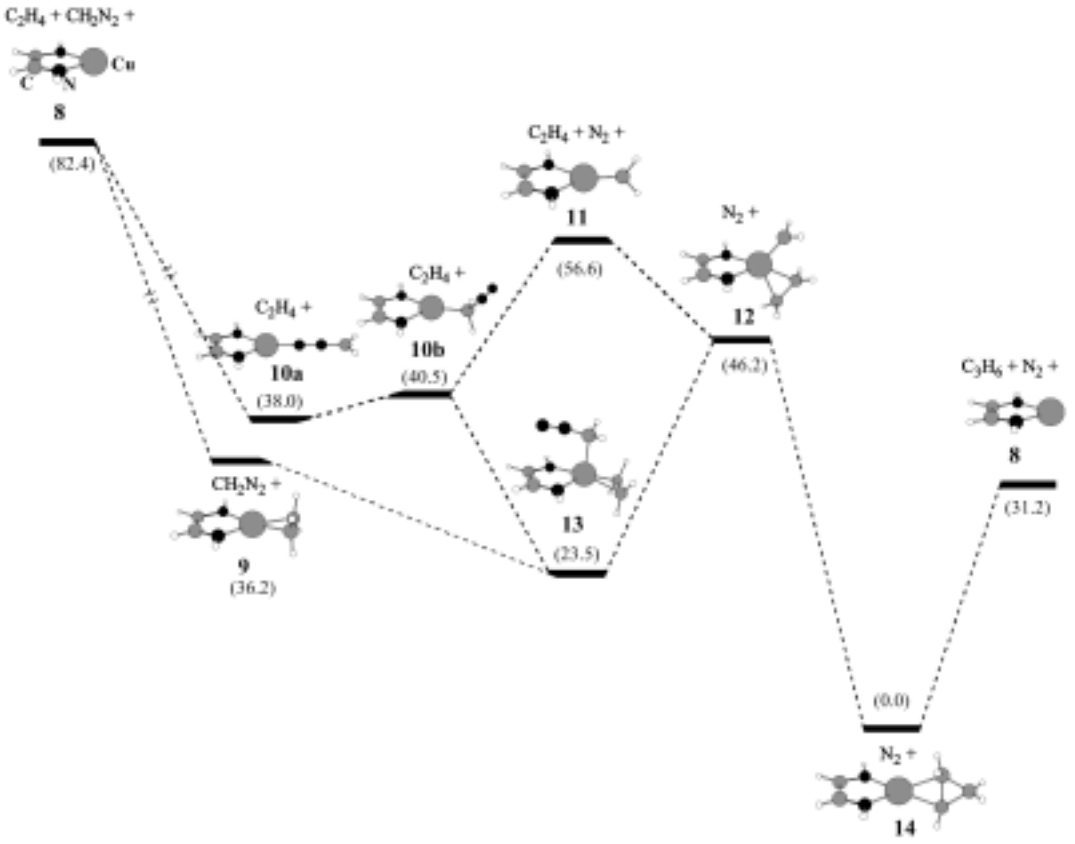

Figure 1. Relevant intermediates on the **3**·Cu^+ + C_2H_4 + CH_2N_2 potential energy surface, together with relative BP86/AE1 energies [kcal/mol] [including zero-point energies (*ZPE*s); see Table 1 for additional thermodynamic data]

Table 1. Thermodynamic data for the intermediates in Figure 1; energies are given in kcal/mol at the BP86/AE1 level

Species	ΔE	$\Delta E + ZPE$	ΔH[a]	ΔG[a]
3·Cu(*c*-C_3H_6)$^+$ + N_2 (**14**)	0.0	0.0	0.0	0.0
3·Cu^+ + C_2H_4 + CH_2N_2 (**8**)	85.4	82.4	82.4	72.4
3·Cu(N_2CH_2)$^+$ + C_2H_4 (**10a**)	39.1	38.0	37.9	38.0
3·Cu(CH_2N_2)$^+$ + C_2H_4 (**10b**)	41.8	40.5	40.5	39.6
3·Cu(CH_2)$^+$ + C_2H_4 + N_2 (**11**)	60.5	56.6	57.0	47.9
3·Cu(C_2H_4)$^+$ + CH_2N_2 (**9**)	37.0	36.2	35.7	36.7
3·Cu(CH_2)(C_2H_4)$^+$ + N_2 (**12**)	48.5	46.2	46.3	47.0
3·Cu(C_2H_4)(CH_2N_2)$^+$ (**13**)	22.6	23.5	22.8	34.4
3·Cu^+ + *c*-C_3H_6 + N_2 (**8**)	31.6	31.2	30.6	23.0

[a] At 298 K.

diate on paths I and II, but the highest points on the two paths, **3**·Cu(CH_2)$^+$ (**11**) and **3**·Cu(CH_2)(C_2H_4)$^+$ (**12**), respectively, are almost equally stable (see ΔG values in the last row of Table 1). A clear-cut distinction between paths I and II is thus very difficult, even for this model system.

In the real systems involving ligands **1** and **2**, side reactions are observed; these involve coupling of the diazo component with itself rather than with the olefin, affording noticeable quantities of fumarate and maleate products (see below, Table 4). Such a process would not be compatible with an exclusive path II type mechanism. Under experimental conditions, the olefin in the olefin-carbene complex can apparently be exchanged with another diazo species, presumably through dissociation and formation of the free carbene.

Even though not directly transferable to the reaction involving large, macrocyclic ligands, the important conclusion from this model study involving **3** as ligand is that Cu(carbene) complexes − in particular, the alkylidene-alkene complex common to both paths studied − are confirmed as viable intermediates. Such carbene complexes are frequently invoked as intermediates, but to the best of our knowledge only two of them have to date been structurally characterized by X-ray diffraction.[4] Where reaction barriers have been specifically computed, they are very similar to reaction energies. Thus, the overall activity should be dictated by the thermodynamic stabilities of the key intermediates. The question is: How do the relevant parts of the potential energy surface change with more realistic ligands and reactants?[2]

2. 2,9-Dimethyl-1,10-phenanthroline Complexes

A ligand more realistic than **3** is 2,9-dimethyl-1,10-phenanthroline (**4**). The recomputation of the potential energy surface corresponding to that with **3** (Figure 1) would be very demanding at the full BP86/AE1 level. It turned out, however, that a less costly approximation, BP86/AE1 single-point energies for BP86/SDD geometries (that is, optimized with a smaller basis set), works very well for key portions of the potential energy surface involving **3** (ΔE values

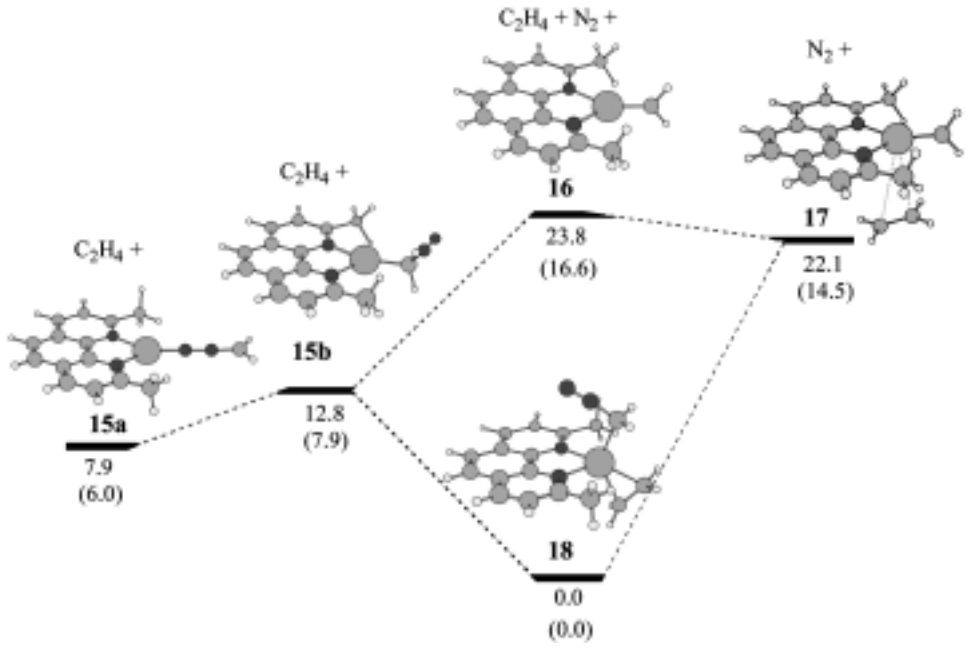

Figure 2. Key intermediates on the **4**·Cu^+ + C_2H_4 + CH_2N_2 potential energy surface, together with relative energies [kcal/mol] from BP86/AE1 single point calculations (in parentheses: B3LYP/AE1 values)

differed by less than 0.2 kcal/mol between BP86 single-point and fully optimized energies). Therefore, only single-point energies with the AE1 basis are discussed below. The results for the key intermediates of paths I and II with **4** as ligands are summarized in Figure 2.

Energies with another density functional, namely the popular B3LYP combination (values in parentheses in Figure 2),[5] were also obtained. The resulting numbers are somewhat dependent on the density functional employed, but the qualitative picture remains the same. One notable difference with the potential energy surface displayed in Figure 1 is that the olefin is bonded to the carbene complex much more weakly with **4** as ligand (note the long Cu···olefin distance in **17**) than with **3** (binding energies ca. 2 vs. 12[6] kcal/mol, respectively). The same is true, though to a lesser extent, for the binding energy of ethene to **4**·$Cu(CH_2N_2)^+$ (**15**) vs. **3**·$Cu(CH_2N_2)^+$ (**10**) (ca. 13 vs. 19[6] kcal/mol). Entropy would be expected to favor olefin dissociation further, which would make paths I and II even less discernible. If anything, the involvement of the free carbene complex is more likely with **4** as ligand than with **3**. Assuming that, as in the case with **3**, barriers on the potential energy surface are similar to reaction energies, a rough estimate for the rate-determining barrier with **4** can be given from

4·$Cu(CH_2N_2)(C_2H_4)^+ \rightarrow$ **4**·$Cu(CH_2)(C_2H_4)^+ + N_2$
ΔE = 22.1 kcal/mol (B3LYP: 14.5).

To be on the safe side, the transition state for formation of the cyclopropane complex from **4**·$Cu(CH_2)(C_2H_4)^+$ (**17**) was located (not shown in Figure 2, but see the substituted derivatives in Figure 3). As with the corresponding complex **3**·$Cu(CH_2)(C_2H_4)^+$ (**12**), the actual cyclopropanation requires only a small additional activation, between 0 (BP86) and 1.8 kcal/mol (B3LYP),[7] affording values for the total barrier of 22.1 (BP86) and 16.3 kcal/mol (B3LYP). The latter value would already be compatible with significant catalytic activity, and the barrier on the free energy surface should be even lower. Indeed, **4** itself has been found to produce active catalysis at room temperature (see below, Table 2).

In order to model the stereoselectivity, it is necessary to introduce substituents both at the olefin and the carbene

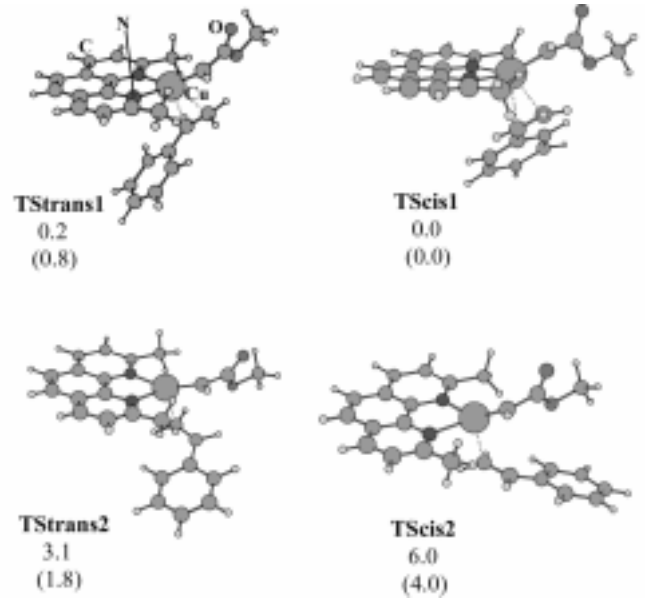

Figure 3. BP86/SDD-optimized transition structures for styrene addition to **4**·$Cu(CHCO_2Me)^+$, producing *trans*- or *cis*-cyclopropane complexes (as indicated by **TStrans** and **TScis**, respectively); relative energies [kcal/mol] from BP86/AE1 single-point calculations are included (in parentheses: B3LYP/AE1 values)

Table 2. Yields and *trans*/*cis* selectivities of cyclopropanations of styrene by ethyl diazoacetate using different copper(I)/2,9-dimethyl-1,10-phenanthroline (Cu^+/**4**) ratios

Cu^+/**4**	no **4**	1:1	1:1.2	1:1.4	1:1.6	1:1.8	1:2
yield [%]	58	67	56	59	62	79	72
trans/*cis*	59:41	61:39	66:34	66:34	66:34	66:34	66:34

moiety. To this end, the four relevant transition states were located for **4**·$Cu(CHCO_2Me)^+$ + styrene. Two of these produce *trans*-cyclopropanes, the other two *cis*-cyclopropanes (Figure 3). The lowest transition states **TStrans1** and **TScis1** (producing *trans* and *cis*, respectively) are quite similar in energy, within 0.2 (BP86) and 0.8 kcal/mol (B3LYP), implying only low or moderate selectivity. Incidentally, the transition structure leading to a *cis* product is computed to be the most stable one. However, the energetic preference is too low for a confident prediction of a slight *cis* preference with ligand **4**.

Subsequently, this system was investigated experimentally (using ethyl diazoacetate rather than methyl diazoacetate). One problem arises here: Unlike the concave 1,10-phenanthrolines such as **1**, the 1,10-phenanthroline-bridged calix[6]arenes **2** and − to an even greater extent − the smaller model ligands **4**−**6** may form 2:1 complexes with copper(I).[8] Thus, it cannot be ruled out that the observed selectivities may be caused by the 1:1 complexes and by free copper(I) [or even by 2:1 complexes; in that case, however, four coordination sites of copper(I) would be occupied and it would be unlikely that this complex would be catalytically active]. The cyclopropanation of styrene with ethyl diazoacetate catalyzed by copper(I) in the presence of 2,9-dimethyl-1,10-phenanthroline (**4**) was therefore investigated using different ligand/copper(I) ratios (see Table 2).

As soon as there is a small excess of ligand **4**, the observed selectivities remain constant. This argues (i) for complete complexation − that is, no more free copper(I) exists, certainly the result of a large binding constant; (ii) then, with increasing amounts of ligand **4**, 2:1 complexes are formed. These must be catalytically inactive as expected; otherwise the constant selectivities with a Cu^+/**4** ratio larger than 1:1 cannot be explained. The equilibrium

$$Cu^+ + 2L \rightleftarrows [CuL]^+ + L \rightleftarrows [CuL_2]^+$$

lies on the side of the 1:1 complex $[CuL]^+$, and the reaction to give Cu^+ and $[CuL_2]^+$ plays no role.

The results in Table 2 demonstrate that there is no evidence for any *cis* selectivity when using **4** as ligand. A typical *trans*/*cis* ratio − 66:34, for ethyl diazoacetate and copper(I) − suggests a small *trans* selectivity, barely exceeding that of free copper(I) (59:41). A possible explanation for the discrepancy between computation and experiment is that the level chosen is not suitable for predicting such small energy differences correctly. It is also possible that not just the relative energies of the transition states are decisive, but rather free energy changes along the whole path. Eventually, molecular dynamics (MD) simulations should be performed to address this question, preferably including solvent molecules.

We note in passing that the two *trans* transition states in Figure 3 would produce enantiomeric products and that they differ in energy between 2.9 (BP86) and 1.0 kcal/mol (B3LYP). These data raise the interesting prospect of simultaneous stereoselectivity and enantioselectivity with suitable chiral ligands, a topical area of research.[1]

3. Complexes with Macrocyclic Ligands

For the more interesting complexes with **1** and **2**, MD simulations in a DFT context are prohibitively expensive. In the hope of finding some clues regarding the origin of the different selectivities, the geometries of **1**·$Cu(CHCO_2Me)^+$ and **2b**·$Cu(CHCO_2Me)^+$ were optimized (RI-BP86/SDD level; that is, including a very time-efficient approximation in the DFT procedure). It is not quite certain to what extent these free carbene complexes would be the actual precursors for the olefin-carbene species prior to cyclopropanation, but the steric conditions should be similar for both types of complexes. The same holds true if, as cannot wholly be ruled out, cyclopropanation occurs in the olefin-diazomethane complexes with simultaneous (possibly concerted) expulsion of N_2.

In any event, a major problem for these flexible macrocycles is the large number of possible energy minima. For **1b**, optimizations were started at the SCF level[9] for each of the four molecules found in the X-ray structure (complex with acetone); the $Cu(CHCO_2Me)^+$ fragment was added to the most stable of the resulting minima, and the structure was fully optimized at the RI-BP86 level (Figure 4, top). The macrocycle adopts a "C_2-tilted", cleft-like conformation. One could imagine the incoming olefin approaching most easily from the opposite side of the carboxy group, such that both substituents would end up *anti*, as is in fact observed.

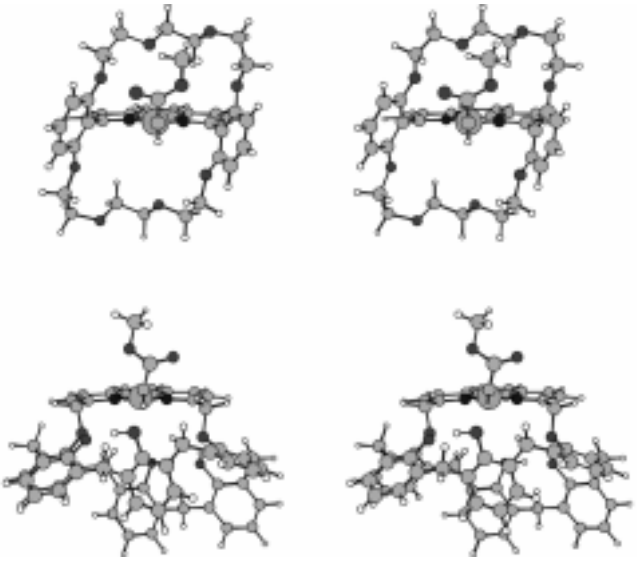

Figure 4. Stereoviews of Cu(carbene) complexes with macrocyclic ligands **1b** (top) and **2b** (bottom), RI-BP86/SDD-optimized (front views)

If this picture is true, the extent and the ease of flexing of the aryl groups attached to the phenanthrolines in the 2,9-positions could be of prime importance for selectivity. In order to assess the conformational flexibility of these aryl groups, we carried out X-ray analyses on a number of 2,9-diaryl-1,10-phenanthrolines. The torsion angles between the plane of the 1,10-phenanthroline moiety and the planes of the aryl rings were determined for a number of arylated 1,10-phenanthrolines **5**−**6**, for bimacrocyclic concave 1,10-phenanthrolines **1**, and also for some metal complexes **7**. In Table 3, these data are compared with the values calculated for **1b**·Cu(CHCO$_2$Me)$^+$ and with data from the literature.[10−13]

Table 3. Torsion angles between the plane of the 1,10-phenanthroline and the planes of the aryl rings in substituted 1,10-phenanthrolines

Compound	Angle [°][a]	Angle [°][b]	Ref. for synthesis
5a	89.5	−	this work
6b	57	62	this work
6c	63	67	[10]
6d	73	77.5	this work
7a	67.5	74	[11]
7b	64−71[c]	74−83[c]	[12]
1a	70	70	[13]
1b[d]	62−66[c] [e]	86[c] [e]	[13]
1b·Cu(CHCO$_2$Me)$^+$[f]	71	72−74	DFT, this work

[a] Torsion angle between the plane of the 1,10-phenanthroline and the first aryl ring. − [b] Torsion angle between the plane of the 1,10-phenanthroline and the second aryl ring. − [c] The aryl ring is distorted; therefore, different values are obtained if the torsion angles are used for various atoms within the two planes. − [d] Host-guest complex with acetone. − [e] Four molecules are found in the unit cell; the extreme values are given. − [f] Pristine cation, RI-BP86/SDD optimized.

According to the X-ray results, the aromatic planes are twisted against one another, but the torsion angle is rather flexible: It can vary from 57° in **6b** to almost 90° in the monoarylated 1,10-phenanthroline **5a**. Remarkably, complexation of two very different metal ions such as copper(II) and palladium(II) does not change these angles. Even in the distorted palladium complex **7b**, angles between 64 and 83° are observed. The DFT-optimized torsion angles in **1b**·Cu(CHCO$_2$Me)$^+$ adopt intermediate values around ca. 73°. The important conclusion from this computation is that the C_2 cleft-like conformation apparent in many solid-state structures is retained in the copper(carbene) complex, a key intermediate in Cu-catalyzed cyclopropanation. Even though the calculations offer no rigorous proof, it is likely that the *trans* selectivity observed with **1b** and related ligands is rooted in this conformational preference.

For **2b**, two isomers ("winged-winged" and "winged-pinched")[14] were optimized and the Cu(CHCO$_2$Me)$^+$ fragment was added to the more stable of these (the "winged-winged" form), followed by a full RI-BP86 optimization. In the course of the optimization, the rigid macrocycle pushes the carbene fragment somewhat out of the phenanthroline plane (Figure 4, bottom, see also Figure 5). The Cu and carbene C atoms lie ca. 0.3 and 0.9 Å above this plane, respectively. The olefin must now approach from the same side as the carboxy group, the opposite hemisphere being blocked by the calixarene belt. An interesting detail of the optimized structure is that the Cu−carbene moiety is also twisted, by ca. 10°, out of the perpendicular arrangement with respect to the Cu−N−N plane (see Figure 4). This twist may be connected with a short contact between the carbene hydrogen atom and one of the phenolic oxygen atoms (1.88 Å). If one assumes that, in the early stage of olefin approach, the olefin substituent will minimize its contacts with both the phenanthroline and the carboxylate moieties, an orientation as sketched in Figure 5 appears likely. Starting with such an orientation, both substituents would end up *cis* in the resulting cyclopropane,[15] consistent with the observed *cis* selectivity with this type of ligand. Full transition state optimizations and/or MD simulations to support this somewhat speculative scenario would be desirable. Unfortunately, such calculations are not yet practically feasible, due to software and hardware limitations. Until these more conclusive computations become available, the optimized structure of **2b**·Cu(CHCO$_2$Me)$^+$ may serve as a starting point for the qualitative rationalization of the observed stereoselectivities as outlined above.

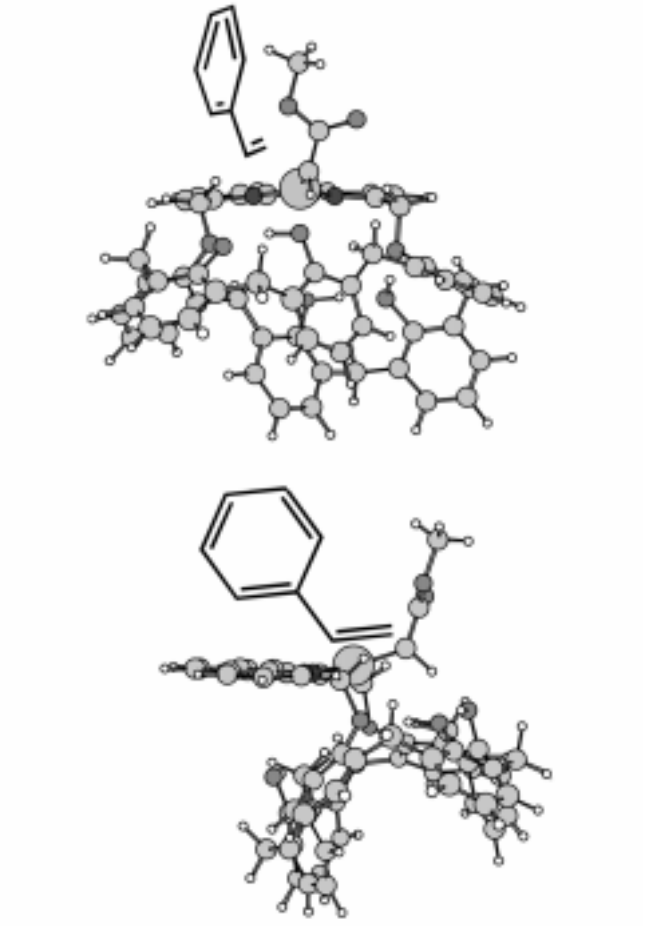

Figure 5. Schematic sketch (front and side views) of the early stages of styrene approach (assumed)

Table 4. Yields and *trans*/*cis* selectivities of cyclopropanations of styrene by ethyl diazoacetate and of the side reaction − the formation of ethyl fumarate and ethyl maleate − using different copper(I)/catalyst (Cu^+/**2a**) ratios

Cu^+/**2a**	no **2a**	1:0.1	1:0.25	1:0.5	1:0.75	1:1	1:1.25	1:1.5	1:2
Yield (*trans* + *cis*) [%]	84	73	86	64	54	70	39	50	62
trans/*cis*	62:38	62:38	57:43	55:45	52:48	32:68	34:66	35:65	35:65
Fumarate/maleate	56:44	50:50	50:50	50:50	50:50	22:78	30:70	26:74	28:72
Yield (fumarate + maleate) [%]	12	11	10	10	8	16	7	9	14

An experimental observation that, at first sight, remains unexplained with this model is the reduced *syn* selectivity when $CHCO_2t$Bu, rather than $CHCO_2$Et, is the carbene moiety. One can argue, however, that the overall selectivity should indeed decrease when the ester and calixarene moieties approach a similar size.

Finally, the *trans*/*cis* selectivities were also determined as a function of the Cu^+/**2a** ratio for the cyclopropanation of styrene by ethyl diazoacetate, catalyzed by **2a**·Cu^+ (see Table 4). Again, the selectivities prove that a 1:1 complex is responsible for the catalysis. Once a ratio of 1:1 is surpassed, *cis* selectivity is found. In parallel to the desired cyclopropanation, coupling of the carbene moieties to form maleates or fumarates always takes place as a side reaction. In the absence of an additional ligand, this side reaction is slightly *trans*-selective. If ligand **2a** is added, the fumarate/maleate ratio also shifts towards *cis*. The parallel increase in the *cis*-cyclopropanes and the *cis*-alkenes argues for the carbene complex as the common intermediate.

Conclusion

Model calculations with **3** and **4** as ligands support a plausible mechanism for Cu-catalyzed olefin cyclopropanation. This mechanism involves Cu(carbene) species, which are confirmed as key intermediates, either free or in the form of complexes with the reactant olefin. The modeling of actual selectivities is difficult, as the slight tendency to promote *cis* cyclopropanation computed for **4** could not be confirmed in subsequent experiments. It should be kept in mind that poor or moderate selectivities (say, of the order of 60:40 to 40:60) are hard to describe theoretically because of the very small energy differences involved. For the macrocyclic ligands **1** and **2**, it is possible to put forward some qualitative explanation of the observed selectivities, based on the DFT-optimized geometries of the carbene complexes. It is proposed that the *trans* selectivity of **1** is a consequence of its C_2-tilted, cleft-like conformation, which was also detected in several solid-state structures of related compounds. The *cis* selectivity of **2** can be rationalized by the fact that, in the corresponding carbene complex, the calixarene macrocycle effectively blocks one hemisphere of the catalyst, thereby favoring relative orientations of the two substituents closer to *syn*-periplanar than to *anti*-periplanar. The remaining challenge for experiment and theory is the design of ligands with enhanced stereoselectivities (and perhaps enantioselectivities) and with lower propensities towards side reactions.

Experimental Section

General: For experimental details see Part 35: U. Lüning, F. Fahrenkrug, M. Hagen, *Eur. J. Org. Chem.*, **2001**, 2161−2163, following paper.

2-(2,6-Dihydroxyphenyl)-1,10-phenanthroline Hydrobromide (5b·HBr): A solution of 2-(2,6-dimethoxyphenyl)-1,10-phenanthroline[10] (7.6 g, 24 mmol) in dry dichloromethane (150 mL) was cooled to −78 °C under nitrogen. A solution of boron tribromide (47.6 g, 189 mmol) in dry dichloromethane (50 mL) was then added slowly, and the mixture was allowed to warm to room temp. and was stirred for additional 48 h. After hydrolysis by dropwise addition of 100 mL of water, the voluminous, slightly yellow precipitate was filtered off, washed three times with 100 mL of dry methanol and dried in vacuo. Remaining boron impurities were distilled off in the form of trimethyl borate. The remaining dark yellow residue was recrystallized from methanol, giving 7.0 g (79%) of **5b**·HBr, m.p. 278 °C (dec.). − IR (KBr): $\tilde{\nu}$ = 3400 cm^{-1} (br., OH), 1618, 1600, 1589, 1560 (arom.), 1270 (C−O). − ^{1}H NMR (250 MHz, [D$_6$]DMSO): δ = 6.56 (d, J = 9 Hz, 2 H, Aryl-H^{3+5}), 7.21 (t, J = 9 Hz, 1 H, Aryl-H^4), 8.02 (dd, J = 9, J = 4.5 Hz, 1 H, Phen-H^8), 8.20 (s, 2 H, Phen-H^{5+6}), 8.74−8.92 (m, 3 H, Phen-H$^{3,4+7}$), 9.19 (dd, $J \approx$ 4.5 Hz, $J \approx$ 1 Hz, 1 H, Phen-H^9). − MS (EI, 70 eV): *m*/*z* (%) = 288 (100) [M − HBr], 287 (94). − $C_{18}H_{13}BrN_2O_2$ (369.21): calcd. C 58.55 H 3.54 N 7.58; found C 58.39 H 3.53 N 7.65.

2-[2,6-Bis(2,2-dimethylpropanoyloxy)phenyl]-1,10-phenanthroline (5a): A mixture of 2-(2,6-dihydroxyphenyl)-1,10-phenanthroline hydrobromide (**5b**·HBr) (1.5 g, 4.0 mmol), pivaloyl chloride (40.0 mL, 325 mmol), and pyridine (20 mL) was heated to reflux for 2 h. After having cooled to room temp., the reaction mixture was poured onto 100 mL of ice/water and was extracted three times with 80 mL of dichloromethane. The combined organic layers were washed three times with 40 mL of 2 N NaOH and twice with 80 mL of water, and dried with $MgSO_4$. After removal of the solvent, the residue was recrystallized from toluene, yielding 1.4 g (78%) of **5a**, m.p. 188 °C. − IR (KBr): $\tilde{\nu}$ = 2960 cm^{-1} (C−H), 1750 (C=O), 1610, 1582, 1545 (arom.), 1105 (C−O). − ^{1}H NMR (250 MHz, [D$_6$]DMSO): δ = 0.88 (s, ca. 18 H, CH_3), 7.11 (d, J = 8 Hz, 2 H, Aryl-H^{3+5}), 7.45 (t, J = 8 Hz, 1 H, Aryl-H^4), 7.63, 7.65 (dd, d, J = 6 Hz, J = 2 Hz, J = 8 Hz, 2 H, Phen-H^{3+8}), 7.85 (s, 2 H, Phen-H^{5+6}), 8.25 (d, J = 8 Hz, 1 H, Phen-H^4), 8.29 (dd, J = 8 Hz, J = 2 Hz, 1 H, Phen-H^7), 9.25 (dd, J = 6 Hz, $J \approx$ 2 Hz, 1 H, Phen-H^9). − MS (EI, 70 eV): *m*/*z* (%) = 456 (37), 372 (100), 288 (73). − $C_{28}H_{28}N_2O_4$ (456.54): calcd. C 73.66 H 6.18 N 6.13; found C 73.48 H 6.15 N 6.19.

X-ray Crystal Structure Determination of 5a: Empirical formula $C_{28}H_{28}N_2O_4$, MW = 456.52 g/mol, colorless plate, a = 10.614 (5), b = 10.881 (5), c = 12.486 (3) Å, α = 79.68 (6), β = 89.79 (4), γ = 61.65 (4)°, V = 1243.0 (9) Å^3, T = 170 K, $\rho_{calcd.}$ = 1.220 g cm^{-3}, μ = 0.08 mm^{-1}, triclinic, space group $P\bar{1}$ (No. 2), Z = 2, CAD4 4-circle diffractometer, Mo-K_α (λ = 0.71073 Å), 4598 measured reflections in the range of 3° ≤ 2θ ≤ 50°, 4345 independent reflections used for refinement and 3335 reflections with $I \geq 2\,\sigma(I)$, R_{int} = 0.0155. Structure solution was performed using SHELXS-86. Structure refinement against F^2 using SHELXL-93. 311 refined parameters, R for all reflections with $I \geq 2\,\sigma(I)$ = 0.0481, wR^2 for all reflections 0.1349, GoF = 1.043, residual electron density 0.44/−0.31 Å^{-3}. All non-hydrogen atoms were refined using anisotropic displacement parameters. The hydrogen atoms were positioned with idealized geometry and refined with isotropic displacement parameters using the riding model. One oxygen atom is disordered and was refined using a split model.

2,9-Bis[2,6-bis(2,2-dimethylpropanoyloxy)phenyl]-1,10-phenanthroline (6b): 2,9-Bis(2,6-dihydroxyphenyl)-1,10-phenanthroline (**6a**)[10] (500 mg, 1.26 mmol) was suspended in dry dichloromethane (15 mL) and dry pyridine (20 mL) under nitrogen. Pivaloyl chloride (1.24 mL, 10.1 mmol) was added with cooling, and the reaction mixture was stirred for 15 h. After hydrolysis with water, the organic layer was washed with a semisaturated solution of sodium carbonate and dried with $MgSO_4$. After removal of the solvent in vacuo, the residue was recrystallized from ethyl acetate, yielding 832 mg (72%) of **6b**, m.p. 310−313 °C. − IR (KBr): $\tilde{\nu}$ = 2960 cm^{-1} (C−H), 1752 (C=O), 1619, 1579, 1543 (arom.), 1459 (CH_3), 1124 (C−O). − ^{1}H NMR (250 MHz, [D$_6$]DMSO): δ = 0.81 (s, 36 H, CH_3), 7.09, 7.09 (d, J = 7.7 Hz, d, J = 8.6 Hz, 4 H, Aryl-H^{3+5}), 7.43 (dd, J = 7.7, J = 8.6 Hz, 2 H, Aryl-H^4), 7.58 (d, J = 8.2 Hz, 2 H, Phen-H^{3+8}), 7.83 (s, 2 H, Phen-H^{5+6}), 8.22 (d, J = 8.2 Hz, 2 H, Phen-H^{4+7}). − MS (EI, 70 eV): m/z (%) = 648 [M$^+$ − C_5H_8O] (100), 564 [M$^+$ − 2 (C_5H_8O)] (10), 480 [M$^+$ − 3 (C_5H_8O)] (6). − MS (CI, isobutane): m/z (%) = 733 [M$^+$ + 1] (100). − $C_{44}H_{48}N_2O_8$·CH_2Cl_2·H_2O (835.85): calcd. C 64.67 H 6.27 N 3.35; found C 64.85 H 5.88 N 3.33.

X-ray Crystal Structure Determination of 6b: Empirical formula $C_{44}H_{48}N_2O_8$, MW = 732.84 g/mol, colorless plate, a = 11.239 (3), b = 19.785 (2), c = 18.722 (2) Å, β = 90.19 (3)°, V = 4163.1 (13) Å^3, T = 170 K, $\rho_{calcd.}$ = 1.169 g cm^{-3}, μ = 0.08 mm^{-1}, monoclinic, space group $P2_1/n$ (No. 14), Z = 4, CAD4 4-circle diffractometer, Mo-K_α (λ = 0.71073 Å), 8371 measured reflections in the range of 3° ≤ 2θ ≤ 50°, 7243 independent reflections used for refinement and 5351 reflections with $I \geq 2\,\sigma(I)$, R_{int} = 0.0144, Structure solution was performed using SHELXS-86. Structure refinement against F^2 using SHELXL-93. 487 refined parameters, R for all reflections with $I \geq 2\,\sigma(I)$ = 0.0495, wR^2 for all reflections 0.1453, GoF = 1.026, residual electron density 0.63/−0.24 Å^{-3}. All non-hydrogen atoms were refined using anisotropic displacement parameters. The hydrogen atoms were positioned with idealized geometry and refined with isotropic displacement parameters using the riding model.

2-(2,6-Dimethoxy-4-methylphenyl)-1,10-phenanthroline (5c): Powdered lithium (1.17 g, 169 mmol) in dry diethyl ether (50 mL) and under argon was activated by action of ultrasound for 30 min. A solution of 4-bromo-3,5-dimethoxytoluene[16] (15.7 g, 67.9 mmol) in dry diethyl ether (200 mL) was then added dropwise and the mixture was heated to reflux for 4 h. A suspension of 1,10-phenanthroline (61 g, 34 mmol) in dry toluene (100 mL) was added and the mixture was heated to reflux for an additional 15 h. After hydrolysis with 200 mL of water and vigorous stirring at room temp. for 45 min, the organic layer was separated and the aqueous layer was extracted three times with 100 mL of dichloromethane. The combined organic layers were washed twice with 100 mL of water and filtered. After evaporation of most of the diethyl ether, MnO_2 (58.4 g, 672 mmol) was added to the remaining toluene solution, and water was distilled off from this mixture for 4 h. After cooling to room temp., the mixture was filtered through a sodium sulfate/Kieselguhr (Celite®) pad, and the solvents were removed in vacuo. The crude product (11.6 g) was used without further purification for the synthesis of **6d.**

2,9-Bis(2,6-dimethoxy-4-methylphenyl)-1,10-phenanthroline (6d): Powdered lithium (0.87 g, 110 mmol) in dry diethyl ether (50 mL) and under argon was activated by action of ultrasound for 30 min. A solution of 4-bromo-3,5-dimethoxytoluene[16] (10.5 g, 45.3 mmol) in dry diethyl ether (130 mL) was then added dropwise and the mixture was heated to reflux for 4 h. A solution of the crude product **5c** (ca. 7.5 g, ca. 23 mmol) in dry toluene (100 mL) was added and the mixture was heated to reflux for an additional 16 h. After hydrolysis with 200 mL of water and vigorous stirring at room temp. for 45 min, the organic layer was separated and the aqueous layer was extracted three times with 100 mL of dichloromethane. The combined organic layer was washed twice with 100 mL of water and filtered. After evaporation of most of the diethyl ether, MnO_2 (38.8 g, 446 mmol) was added to the remaining toluene solution, and water was distilled off from this mixture for 4 h. After cooling to room temp., the mixture was filtered through a sodium sulfate/Kieselguhr (Celite®) pad, and the solvents were removed in vacuo. Chromatography [silica gel, dichloromethane/ethanol (15:1)] gave 1.6 g of **6d** (ca. 39%, calculated on 1,10-phenanthroline), m.p. 277−278 °C. − IR (KBr): $\tilde{\nu}$ = 2936 cm^{-1} (CH_3), 2836 (OCH_3), 1609, 1578 (conj. cycl. C=N−), 1234, 1125 (C−O), 855, 815 (arom. C−H). − ^{1}H NMR (500 MHz, $CDCl_3$): δ = 2.37 (t, J = 0.7 Hz, 6 H, CH_3), 3.70 (s, 12 H, OCH_3), 6.47 (d, J = 0.8 Hz, 4 H, Aryl-H^{3+5}), 7.60 (d, J = 8.2 Hz, 2 H, Phen-H^{3+8}), 7.76 (s, 2 H, Phen-H^{5+6}), 8.20 (d, J = 8.2 Hz, 2 H, Phen-H^{4+7}). − ^{13}C NMR (125 MHz, $CDCl_3$, gated): δ = 22.2 (q, CH_3), 56.4 (q, OCH_3), 105.9 (d, Aryl-C^{3+5}), 118.0 (s, Aryl-C^1), 126.0 (d, Phen-C^{3+8}), 126.1 (d, Phen-C^{5+6}), 127.4 (s, Phen-C^{5a+6a}), 135.2 (d, Phen-C^{4+7}), 139.9 (s, Aryl-C^4), 146.3 (s, Phen-C^{10a+b}), 154.9 (s, Phen-C^{2+8}), 158.2 (s, Aryl-C^{2+6}). − MS (EI, 70 eV): m/z (%) = 479.4 (100) [M$^+$ − H], 462.4 (34), 449.4 (23) [M$^+$ − CH_2O], 431.3 (14). − MS (CI, isobutane): m/z (%) = 481 (100) [M$^+$ + 1]. − HR-MS (EI, 70 eV): m/z (%) = $C_{30}H_{27}N_2O_4$: found 479.2011; calcd. 479.1971 (diff. = −8.4 ppm). − $C_{30}H_{28}N_2O_4$: found 480.2056; calcd. 480.2049 (diff. = −1.5 ppm). − $C_{29}{}^{13}CH_{27}N_2O_4$: found 481.2077; calcd. 481.2083 (diff. = 1.1 ppm).

X-ray Crystal Structure Determination of 6d: Empirical formula $C_{30}H_{28}N_2O_4$·2 CH_3OH·H_2O, MW = 562.64 g/mol, colorless block, a = 8.2800 (5), b = 12.091 (1), c = 16.570 (1) Å, α = 108.05 (1), β = 94.66 (1), γ = 106.94 (1)°, V = 1481.8 (2) Å^3, T = 150 K, $\rho_{calcd.}$ = 1.261 g cm^{-3}, μ = 0.09 mm^{-1}, triclinic, space group $P\bar{1}$ (No. 2), Z = 2, STOE Imaging Plate Diffraction System (IPDS), Mo-K_α (λ = 0.71073 Å), 10587 measured reflections in the range of 3° ≤ 2θ ≤ 52°, 5323 independent reflections used for refinement and 4546 reflections with $I \geq 2\,\sigma(I)$, R_{int} = 0.0336. Structure solution was performed using SHELXS-86. Structure refinement against F^2 using SHELXL-93. 403 refined parameters, R for all reflections with $I \geq 2\,\sigma(I)$ = 0.0425, wR^2 for all reflections 0.1250, GoF = 1.056, residual electron density: 0.23/−0.18 Å^{-3}. All non-hydrogen atoms were refined using anisotropic displacement parameters. The hydrogen atoms were positioned with idealized geometry and refined with isotropic displacement parameters using the

riding model. The oxygen atom of one ethanol molecule is disordered and was refined using a split model.

Crystallographic data (excluding structure factors) for the structure(s) reported in this paper have been deposited with the Cambridge Crystallographic Data Centre as supplementary publication no. CCDC-157321 (**5a**), -157320 (**6b**), and -157322 (**6d**). Copies of the data can be obtained free of charge on application to CCDC, 12 Union Road, Cambridge CB2 1EZ, UK [Fax: (internat.) + 44-1223/336-033; E-mail: deposit@ccdc.cam.ac.uk].

Computations: For complexes with model ligand **3**, geometries were optimized, using symmetry constraints if appropriate, at the BP86/AE1 level, employing the exchange and correlation functionals of Becke[17] and Perdew,[18] respectively, together with a fine integration grid (75 radial shells with 302 angular points per shell), augmented Wachters' basis[19] on Cu (8s7p4d), and 6−31G*[20] basis on all other elements. The nature of the stationary points was verified by computations of the harmonic frequencies at that level. Transition states were characterized by a single imaginary frequency, and visual inspection of the corresponding vibrational modes ensured that the desired minima were connected. This and comparable DFT levels have proven quite successful for transition metal compounds [including copper(ethene)[21] and copper(diazomethane) complexes][22] and are well suited for the description of structures, energies, barriers etc.[23] For complexes with the ligands **4**, geometries were optimized at the BP86/SDD level, using Stuttgart−Dresden relativistic effective core potentials[24,25] with somewhat smaller valence basis sets, Cu (6s5p3d),[24] C, N, O (2s2p),[25] and a double-zeta basis on H.[26] Energies were computed for these geometries at the BP86/AE1 level and, in addition, at the B3LYP/AE1 level; i.e., using the exchange-correlation functionals according to Becke (hybrid),[27] and Lee, Yang, and Parr.[28] It was checked, using selected complexes of ligand **3**, that relative energies obtained with such BP86/AE1 single-point calculations were very similar to fully optimized BP86/AE1 data. All these computations were performed with the Gaussian 98 program package.[29] For the complexes with the larger macrocyclic ligands, **1b** and **2b**, geometries were optimized at the BP86/SDD level, using the RI (resolution of identity) approximation as implemented[30] in TURBOMOLE,[31] together with a medium-sized grid (grid 3).[32] The optimizations were effected using ChemShell[33] and a suitable combination of Cartesian and hybrid delocalized internal coordinates.[34]

Synthesis and Determination of Selectivity: Under nitrogen or argon, copper(I) triflate hemi-benzene complex (Aldrich, ca. 10.0 mg, 39.7 μmol) was placed in a vial sealed with a Teflon septum and was weighed with an accuracy of ± 0.1 mg. Styrene (17.5 mmol) and the corresponding amount of ligand **2a** or **4**, dissolved in 1,2-dichloroethane (4 mL) (ligand/copper ratio from 0.1:1 up to 2:1, see Tables 3 and 4) was then added. Dissolution was aided with ultrasound. The diazoacetate (2 mmol) was then carefully added with a syringe. Nitrogen was usually evolved rapidly. After 24 h, the copper salt was removed by filtration through silica gel (5 × 3 cm, 150 mL of diethyl ether). After concentration to ca. 5 mL, the flask was filled to 25 mL with 1,2-dichloroethane and *n*-hexadecane was added as GC standard (4.0 mg/ml). GC analysis: SE30 or Optima 1/25 m, 80 °C for 5 min, 10 °C/min until 140 °C, 1 min, 2 °C/min until 160 °C, 1 min, 20 °C/min until 240 °C, 2 min.

Acknowledgments

M. B. wishes to thank Prof. Dr. W. Thiel for his continuous support and the Deutsche Forschungsgemeinschaft for a Heisenberg fellowship. Calculations were carried out with Compaq XP1000 and ES40 workstations at the Max-Planck-Institut, Mülheim.

[1] Recent reviews: [1a] M. P. Doyle; M. A. McKervey, T. Ye, *Modern Catalytic Methods for Organic Synthesis with Diazo Compounds: From Cyclopropanes to Ylides*, Wiley & Sons, New York, Chichester, Weinheim, Brisbane, Singapore, Toronto, **1998**. – [1b] A. Pfaltz, *J. Heterocycl. Chem.* **1999**, *36*, 1437−1451.−[1c] R. C. Hartley, S. T. Caldwell, *J. Chem. Soc., Perkin Trans. 1* **2000**, 477−501.−[1d] J. S. Johnson, D. A. Evans, *Acc. Chem. Res.* **2000**, *33*, 325−335. − More recent work: [1e] M. J. Fernandez, J. M. Fraile, J. I. Garcia, J. A. Mayoral, M. I. Burguete, E. Garcia-Verdugo, S. V. Luis, M. A. Harmer, *Top. Catal.* **2000**, *13*, 303−309.−[1f] T. Niimi, T. Uchida, R. Irie, T. Katsuki, *Tetrahedron Lett.* **2000**, *41*, 3647−3651.−[1g] M. Glos, O. Reiser, *Org. Lett.* **2000**, *2*, 2045−2048.−[1h] R. Boulch, A. Scheurer, P. Mosset, R. W. Saalfrank, *Tetrahedron Lett.* **2000**, *41*, 1023−1026.−[1i] D. J. Cho, S. J. Jeon, H. S. Kim, C. S. Cho, S. C. Shim, T. J. Kim, *Tetrahedron: Asymmetry* **1999**, *10*, 3833−3848.−[1j] G. Chelucci, M. G. Sanna, S. Gladiali, *Tetrahedron* **2000**, *56*, 2889−2893.−[1k] V. K. Aggarwal, H. W. Smith, G. Hynd, R. V. H. Jones, R. Fieldhouse, S. E. Spey, *J. Chem. Soc., Perkin Trans. 1* **2000**, 3267−3276.−[1l] A. Abiko, J.-F. Liu, G. Wang, S. Masamune, *Tetrahedron Lett.* **1997**, *38*, 3261−3264.−[1m] F. Löffler, M. Hagen, U. Lüning, *Synlett* **1999**, 1826−1828; and ref. cited in the above publications.

[2] No solvent effects were computed in the present study. It is unlikely, however, that the weakly coordinating solvents (such as 1,2-dichloroethane) used in the experiments would induce such a radical change in the mechanism as to invalidate our more qualitative conclusions.

[3] Such a dissociative process might be assisted to some extent by the solvent, a possibility that was, however, not explored further in this study.

[4] [4a] H. G. Raubenheimer, S. Cronje, P. H. van Rooyen, P. J. Olivier, J. G. Toerien, *Angew. Chem.* **1994**, *106*, 687−688; *Angew. Chem. Int. Ed. Engl.* **1994**, *33*, 672−673. − [4b] H. G. Raubenheimer, S. Cronje, P. J. Olivier, *J. Chem. Soc., Dalton Trans.* **1995**, 313−316.

[5] Even though the B3LYP combination has proven to be quite accurate for thermodynamic data of first- and second-row compounds, its general superiority over other functionals is much less clear in the case of transition metal complexes; geometries of the latter, at least, appear to be better described with non-hybrid functionals such as BP86 (see for instance ref.[23]). The B3LYP data have been included to assess the sensitivity of the results to a particular choice of the density functional.

[6] Values of ΔE from Table 1 − i.e., without zero-point correction − employed. Note that these binding energies are probably upper limits since they are not corrected for basis set superposition error.

[7] It cannot be ruled out that, for the larger macrocyclic ligands, additional steric effects capable of modifying this extra activation might come into play.

[8] F. Löffler, U. Lüning, G. Gohar, *New J. Chem.* **2000**, *24*, 935−938.

[9] These preliminary optimizations were performed on the lowest ab initio level, the Hartree−Fock self-consistent field. This level is appropriate for main group organic compounds, but not for transition metal complexes.

[10] U. Lüning, M. Müller, *Chem. Ber.* **1990**, *123*, 643−645.

[11] M. Gelbert, Ph. D. thesis, Freiburg, **1995**.

[12] B. Meynhardt, U. Lüning, C. Wolff, C. Näther, *Eur. J. Org. Chem.* **1999**, 2327−2335.

[13] U. Lüning, M. Müller, M. Gelbert, K. Peters, H. G. von Schnering, M. Keller, *Chem. Ber.* **1994**, *127*, 2297−2306.

[14] For other A,D-bridged calix[6]arenes, a half-winged/half-pinched conformation has been calculated first in: U. Lüning, H. Ross, I. Thondorf, *J. Chem. Soc., Perkin Trans. 2* **1998**, 1313−1317.

[15] A *cis*-cyclopropane would also arise if the styrene approached with the same orientation as depicted in Figure 5, but from the "other side" of the carboxylate group; that is, from the quadrant with the carbonyl oxygen atom.
[16] J. Gunziner, R. Tabacchi, *Helv. Chim. Acta* **1985**, *68*, 1940−1947.
[17] A. D. Becke, *Phys. Rev. A* **1988**, *38*, 3098−3100.
[18] [18a] J. P. Perdew, *Phys. Rev. B* **1986**, *33*, 8822−8824. − [18b] J. P. Perdew, *Phys. Rev. B* **1986**, *34*, 7406.
[19] [19a] A. J. H. Wachters, *J. Chem. Phys.* **1970**, *52*, 1033−1036. − [19b] P. J. Hay, *J. Chem. Phys.* **1977**, *66*, 4377−4384.
[20] [20a] W. J. Hehre, R. Ditchfield, J. A. Pople, *J. Chem. Phys.* **1972**, *56*, 2257−2261. − [20b] P. C. Hariharan, J. A. Pople, *Theor. Chim. Acta.* **1973**, *28*, 213−222.
[21] R. H. Hertwig, W. Koch, D. Schröder, H. Schwarz, J. Hrušák, P. Schwerdtfeger, *J. Phys. Chem.* **1996**, *100*, 12253−12260.
[22] Q. Cui, D. G. Musaev, M. Svensson, K. Morokuma, *J. Phys. Chem.* **1996**, *100*, 10936−10944.
[23] See for instance: W. Koch, M. C. Holthausen, *A Chemist's Guide to Density Functional Theory*, Wiley-VCH, Weinheim, **2000**, and the extensive bibliography therein.
[24] D. Andrae, U. Häußermann, M. Dolg, H. Stoll, H. Preuß, *Theor. Chim. Acta* **1990**, *77*, 123−141.
[25] A. Bergner, M. Dolg, W. Küchle, H. Stoll, H. Preuß, *Mol. Phys.* **1993**, *80*, 1431−1441.
[26] T. H. Dunning, *J. Chem. Phys.* **1970**, *53*, 2823−2833.
[27] A. D. Becke, *J. Chem. Phys.* **1993**, *98*, 5648−5642.
[28] C. Lee, W. Yang, R. G. Parr, *Phys. Rev. B* **1988**, *37*, 785−789.
[29] M. J. Frisch, G. W. Trucks, H. B. Schlegel, G. E. Scuseria, M. A. Robb, J. R. Cheeseman, V. G. Zakrzewski, J. A. Montgomery, R. E. Stratman, J. C. Burant, S. Dapprich, J. M. Milliam, A. D. Daniels, K. N. Kudin, M. C. Strain, O. Farkas, J. Tomasi, V. Barone, M. Cossi, R. Cammi, B. Mennucci, C. Pomelli, C. Adamo, S. Clifford, J. Ochterski, G. A. Petersson, P. Y. Ayala, Q. Cui, K. Morokuma, D. K. Malick, A. D. Rabuck, K. Raghavachari, J. B. Foresman, J. Cioslowski, J. V. Ortiz, A. G. Baboul, B. B. Stefanov, C. Liu, A. Liashenko, P. Piskorz, I. Komaromi, R. Gomperts, R. L. Martin, D. J. Fox, T. Keith, M. A. Al-Laham, C. Y. Peng, A. Nanayakkara, C. Gonzalez, M. Challacombe, P. M. W. Gill, B. G. Johnson, W. Chen, M. W. Wong, J. L. Andres, C. Gonzales, M. Head-Gordon, E. S. Replogle, J. A. Pople, *Gaussian98*, Gaussian, Inc., Pittsburgh PA, **1998**.
[30] [30a] K. Eichkorn, O. Treutler, H. Öhm, M. Häser, R. Ahlrichs, *Chem. Phys. Lett.* **1995**, *240*, 283−289. − [30b] K. Eichkorn, O. Treutler, H. Öhm, M. Häser, R. Ahlrichs, *Chem. Phys. Lett.* **1995**, *242*, 652−660.
[31] R. Ahlrichs, M. Bär, M. Häser, H. Horn, C. Kölmel, *Chem. Phys. Lett.* **1989**, *162*, 165−169.
[32] O. Treutler, R. Ahlrichs, *J. Chem. Phys.* **1995**, *102*, 346−354.
[33] P. Sherwood, A. H. deVries, *ChemShell − A Shell for Computational Chemistry*, CCLRC Daresbury Laboratory, **1999**; see http://www.dl.ac.uk
[34] S. R. Billeter, A. J. Turner, W. Thiel, *Phys. Chem. Chem. Phys.* **2000**, *2*, 2177−2186.

Received November 28, 2000
[O00600]